J Mater Sci: Mater Med (2010) 21:1655–1663
DOI 10.1007/s10856-010-4014-8

Influence of Fe(II) and Fe(III) on the expression of genes related to cholesterol- and fatty acid metabolism in human vascular smooth muscle cells

Andreas Drynda · René Hoehn · Matthias Peuster

Received: 13 October 2009 / Accepted: 28 January 2010 / Published online: 17 February 2010

Abstract Iron is the major alloy component for a large variety of cardiovascular devices such as stents. In recent studies it has been shown that biodegradable iron or iron based stents exhibit good mechanical features with no pronounced neointimal proliferation. Whole genome gene profiling using DNA chip technology revealed that genes involved in cholesterol and fatty acid metabolism (low-density lipoprotein receptor, LDL-R; 3-hydroxy-3-methylglutaryl-Coenzyme A synthase 1 (HMGCS1) and fatty acid desaturase 1 (FADS1) are up-regulated after exposure of vascular smooth muscle cells with soluble ferrous iron. To analyze the effects of iron on these genes in detail we co-incubated human vascular smooth muscle cells for 12 and 24 h with different concentrations of ferrous (soluble iron(II)-gluconate) and ferric iron (soluble iron(III)-chloride), Ferrlecit^{TM}, a commercially available drug (ferric iron-gluconate complex) and solid iron coils. The expression of LDL-R, HMGCS1 and FADS1 was analyzed using TaqMan® Real-time PCR. After 24 h, all forms of iron led to a significant up-regulation of the examined genes. At high concentrations the expression rates declined, probably as a result of reduced metabolic activity. The most prominent effects were observed after co-incubation with Ferrlecit^{TM}, probably caused by an increased bioavailability of the iron gluconate complex. We postulate that both, bi- and trivalent forms of iron induce the expression of LDL-R, HMGCS1 and FADS1 by generation of highly reactive oxygen species. Further animal experiments using tissues from iron-stented vessels may lead to a more profound insight into iron induced expression of cholesterol- and fatty acid metabolism related genes.

A. Drynda · R. Hoehn
Department of Pediatric Cardiology and Intensive Care, Children's Hospital, University of Rostock, Rembrandtstraße 16/17, 18057 Rostock, Germany

M. Peuster (✉)
Department of Pediatrics, Comer Children's Hospital, University of Chicago, 5721 S Maryland Ave, Chicago, IL 60637, USA
e-mail: mpeuster@peds.bsd.uchicago.edu

1 Introduction

Iron is an important component of various biomedical alloys used for cardiovascular applications [1–3]. For a long time biomedical implants produced from a variety of metals including AISI (American Iron and Steel Institute) 316-L, Nitinol and tungsten were considered to be non-corrosive. Recently it has been shown, that corrosion of biomedical implants is abundant in physiological environments [4–7].

Cardiovascular stents are used to avoid the recoil of obstructed vessels or to treat vessel dissections that occur during angioplasty. A variety of indications for the implantation of cardiovascular stents exist. These include coarctation or re-coarctation of the aorta, peripheral pulmonary stenoses, systemic venous stenoses and ductal stenting. The use of stents in pediatric patients however, is limited by the growth of the vessels adjacent to the stent. Growth-related re-stenosis at the implantation site may therefore necessitate further interventions to adapt the stent diameter to the diameter of the vessel adjacent to the implantation site. The use of biodegradable stents could overcome these limitations [8]. Recently, magnesium-based alloys have been introduced which exhibit adequate short-term biocompatibility. However, the use was complicated by the lack of radiopacity, inferior mechanical properties in comparison to currently available stents and

significant calcifications in the vessel wall due to the rapid degradation process [9]. Therefore, efforts are made to reduce the corrosion rate by modification of the composition of magnesium-based alloys or surface treatments [10].

Although medical stainless steel alloys (e.g. AISI 316-L) corrode under in vivo conditions [7] their degradation rate is low. Complete degradation can not be expected to occur within a normal life expectancy of a patient, even if treated at a very young age [11]. With the intention to use a more rapid corrosion as a concept of biodegradation, pure iron was used for the first bio-corrodible iron stent in 2001 [12]. Pure iron has a lot of beneficial properties compared with other metals or alloys. Since iron is an essential part of several enzymes and sophisticated transport systems for the iron homeostasis exist, the clearance of iron and its corrosion products is ensured so that systemic toxicity is unlikely to occur [13]. Furthermore, in vivo studies using minipigs have shown that biodegradation of iron stents was not associated with an increased neointimal proliferation or inflammation of the stented vessel [1]. In vitro, these results were confirmed by cell culture experiments using human vascular smooth muscle cells (SMC) co-incubated with soluble iron(II) [14]. Furthermore, gene expression profiling (Affymetrix Chip technology) suggested, that soluble iron(II) ions induce the expression of cell cycle derived genes as well as genes involved in cholesterol and lipid metabolism.

The gene expression profiles obtained from Affymetrix chip analysis are predominantly of qualitative nature. Although fold changes related to control samples can be calculated their quantitative significance is rather poor. Therefore, the aim of this study, was to confirm and quantify the data derived from the Affymetrix gene expression experiments by TaqMan® Real-time PCR. We focussed on selected genes involved in the synthesis of cholesterol fatty acid metabolism: low density lipoprotein receptor (LDL-R), 3-hydroxy-3-methylglutaryl-Coenzyme A synthase 1 (HMGCS1) and fatty acid desaturase 1 (FADS1).

Besides soluble iron(II) and iron(III) ions, the influence of particle-based forms of iron on gene expression was also investigated. For this purpose SMCs were also co-incubated with Fe(III) in a Fe_2O_3 gluconate-complex (commercial available as Ferrlecit™, used for the treatment of iron-deficiency diseases), as well as solid iron in form of coils prepared from twisted wires.

2 Materials and methods

2.1 Isolation and cultivation of primary cells

Primary human vascular smooth muscle cells (SMCs) were isolated from umbilical veins according to standard protocols [15]. The purity of the SMCs was assessed by immunohistochemistry, using a primary mouse anti-human antibody (Dako M0851, Dako, Hamburg, Germany) and a secondary dye-labelled goat anti-mouse antibody (Alexa 488, Invitrogen, Karlsruhe, Germany). The cells from several individuals were pooled to account for unavoidable variations in geno- and phenotype. Reproducibility was ensured by storing cell culture aliquots in liquid nitrogen until use. After thawing the SMCs were cultivated in SmGM medium (SmGM-2-Bulletkit, orderID#CC-3182, Lonza, Switzerland), containing 5% FBS (fetal bovine serum), gentamicin-sulphate, amphotericin B, hFGF-β (human fibroblast growth factor-β) and hEGF (human epidermal growth factor), at 37°C in a humidified 5% CO_2 atmosphere. For cell culture experiments the SMCs were used up to passage 10.

2.2 Determination of metabolic competence

For the detection of metabolic competence, SMCs (5×10^3 each well) were incubated with iron(II) gluconate, iron(III) chloride and Ferrlecit™ (Sanofi-Aventis, Germany). Metabolic activity of the exposed cells was measured using the WST-1 test (Roche, Germany orderID#1644807). The principle of this test depends on the cleavage of the tetrazolium salt (4-[3-(4-Iodophenyl)-2-(4-nitrophenyl)-2H-5-tetrazolio]-1,3-benzene disulfonate) to formazan, by mitochondrial dehydrogenases. The increase of enzyme activity leads to an increase in the amount of formazan dye formed, which correlates with the number of metabolically active cells in the culture. After 24, 72, 144 and 240 h the cell culture medium was removed and replaced by 100 µl medium containing 10% of the WST-1 reagent. After an incubation period of 2 h (37°C, humidified 5% CO_2 atmosphere) the optical density (OD) at 440 nm was determined relative to a reference OD at 650 nm using an ELISA multiplate reader (Sunrise, Tecan). The background was adjusted using 100 µl of each medium, containing 10% WST-1 reagent without cells.

2.3 Cell count

Cells were incubated in duplicates on 96-well plates (5×10^3 each) and stimulated with iron(II)-gluconate, iron(III)-chloride and Ferrlecit™. After each time point (6 and 24 h) cells were washed with Dulbeccos PBS (1×) to remove non adherent dead or metabolic limited cells, trypsinized with 50 µl trypsin (PAA, Austria) and then pooled. The undiluted cell suspension was counted in a Neubauer chamber. Results, obtained as the mean value of the four major squares, were expressed as the "relative number of metabolically active cells".

Table 1 Target genes and TaqMan® assays used for quantitative Real-time-PCR

Gene	ID#*	RefSeq	Amplicon lengths (bp)
Glyceraldehyde-3-phosphate dehydrogenase (GAPDH)	Hs99999905_m1	NM_002046.3	122
Low-density lipoprotein receptor (LDL-R)	Hs00181192_m1	NM_000527.3	61
3-hydroxy-3-methylglutaryl-Coenzyme A synthase 1 (HMGCS1)	Hs00266810_m1	NM_002130.6	120
Fatty acid desaturase 1 (FADS1)	Hs00203685_m1	NM_013402.4	77

* The extension m1 of the ID numbers denotes, that the assays have exon–intron boundaries and are specific for cDNA amplification

2.4 Gene expression analysis

For quantitative gene expression experiments 4×10^5 SMCs per 3 ml medium were seeded in 6-well cell culture plates (Corning, Netherlands) and incubated for 12 and 24 h with different concentrations (30, 50, 100, 500 1000 μg/ml) of the iron(II)-chloride, iron(III)-chloride or Ferrlecit™ (Sanofi-Aventis, Germany) under standard conditions. Beside these "soluble" iron compounds the SMCs were also incubated with solid iron. For this purpose iron coils prepared of twisted tempered iron wires (length: 6 cm, diameter: 0.25 mm, approx. 46 mg, Goodfellow, Cambridge, UK) were placed carefully onto the cells layers (also 6-well plates).

After 12 or 24 h, the cells were harvested and total RNA was isolated (RNeasy Mini Kit, Qiagen, Hilden, Germany) according to the manufacturer's instructions. Quantity and quality of RNA were determined using the Nanodrop technology (Nanodrop ND-1000, Peqlab, Erlangen, Germany) with OD_{260}/OD_{280} ratios of 1.9–2.1. Additionally, RNA quality was analyzed on an Agilent 2100 Bio analyzer (Agilent, Böblingen, Germany) with respect to 18S and 28S ribosomal RNA (Lab-on-a-chip RNA 6000 Nano kit). An additional on-column DNAse digestion was not performed, because all used TaqMan® gene-expression assays were designed with exon–intron boundaries, amplifying only cDNA. 1 μg of total RNA was used for reverse transcription with Maloney murine leukemia virus transcriptase in a final volume of 20 μl using the "ABI High capacity cDNA transcription Kit (Applied Biosystems, Darmstadt, Germany) according to the manufacturers instructions.

Real-time PCR for gene expression analysis was performed on an ABI 7500 Sequence Detection System (Applied Biosystems, Darmstadt, Germany), using a 2-step PCR protocol and a reaction volume of 10 μl performed as triplicates. After an initial denaturating step (95°C, 10 min) the cDNA was amplified with 40 cycles. Cycle parameters were 95°C for 15 s and 60°C for 1 min. TaqMan® primer/probes sets for the genes to be analyzed were obtained as 20-fold concentrated, ready to use, solutions (ABI, Darmstadt, Germany). The ID-numbers, reference sequences, context sequences of the probes and amplicon lengths of the used gene expression assays are summarized in Table 1. Expression data were generated by relative quantification ($\Delta\Delta C_t$ method). For this purpose, the cDNA was amplified with the appropriate primers and probes for the target genes as well as for the housekeeping gene GAPDH which is expressed constitutively in exposed as well as in control cells, and is used to normalize different amounts of RNA. One assumption of the $\Delta\Delta C_t$ method is that all PCR reactions (GAPDH and the targets) have the same efficiency.

The C_t values of GAPDH were subtracted from the C_t's of the gene targets (ΔC_t). To refer samples incubated with bi- and trivalent iron ions, Ferrlecit™ or solid iron to the control cells the ΔC_t value of the control was subtracted from all other samples, also from itself ($\Delta\Delta C_t$). $\Delta\Delta C_t$ values <0 represent up-regulation, $\Delta\Delta C_t$ values >0 down-regulation of gene expression.

2.5 Analysis of data

Determination of metabolic activity was performed in quintuplicates. From five independent readings the median was calculated with the corresponding standard deviation. The cell count experiments were performed in duplicates.

For gene expression analysis the cell culture experiments were repeated three times. TaqMan® Real-Time PCR was carried out in triplicates with an accepted standard deviation of 0.15 C_t values. All data were analyzed using standard statistical software. *P* value of less than 0.05 were regarded as significant.

3 Results

In a first set of experiments the toxicity potential of iron(II) gluconate, iron(III) chloride and Ferrlecit™ on smooth muscle cells was investigated. Therefore the metabolic activity, a key parameter of cell viability, was analyzed using the colometric WST-1 test. The influence of iron(II) gluconate on smooth muscle cells is displayed in Fig. 1a for 6 and 24 h (lower set of graphs, left y-axis). The data indicate, that iron(II) gluconate leads to a decrease in metabolic activity of SMCs in a dose-dependent fashion

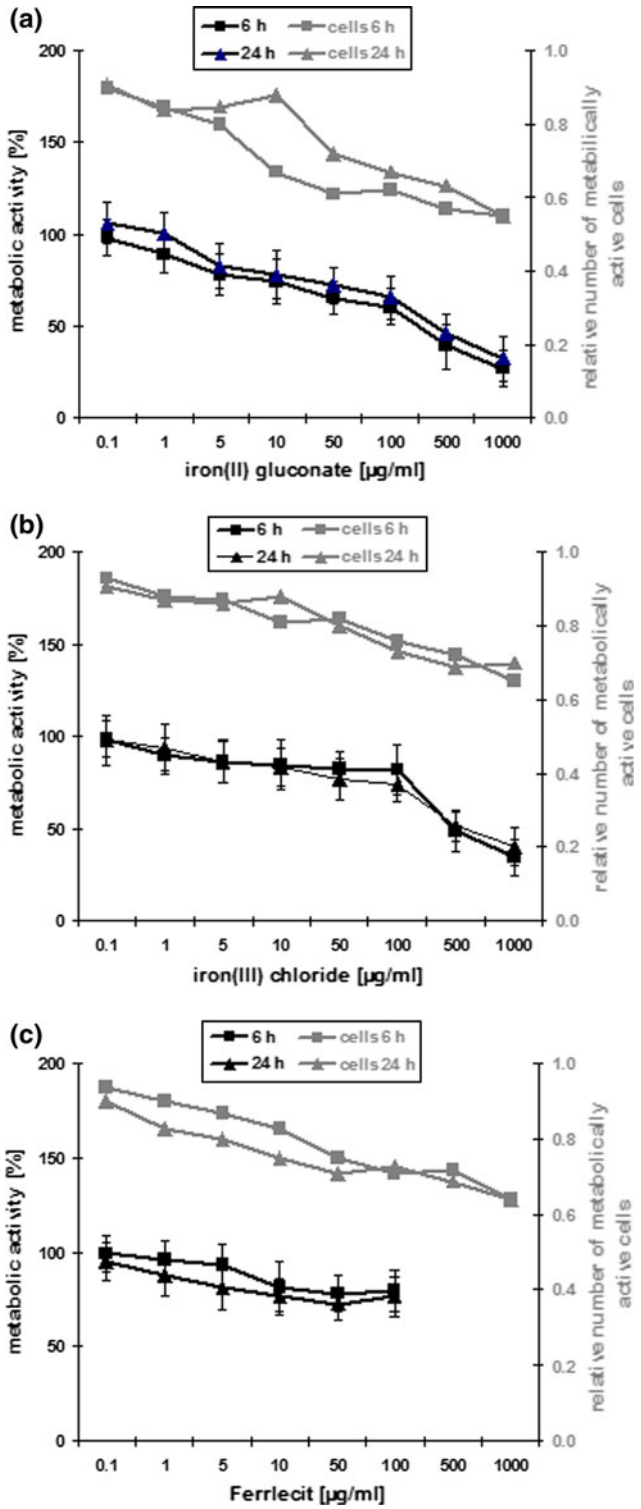

◀**Fig. 1** Human vascular smooth muscle cells (5×10^3 each) were incubated with iron(II) gluconate (**a**), iron(III) chloride (**b**) and Ferrlecit™ (**c**) in a concentration range from 0.1 to 1,000 µg/ml. The metabolic activity was measured after 6 and 24 h using the colorimetric WST-1 test (lower part of the figure, left y-axis). The data were calculated as percentage related to control cells. The upper part of the figure displays the relative number of metabolically active cells, (*grey lines*, right y-axis). With regard to metabolic activity all indicated data points are mean values of five independent measurements

down to a minimal 25% at a Fe(II) concentration of 1 mg/ml. The relative number of metabolically active cells decreased dose-dependently for all time points (upper set of graphs, right y-axis).

The co-incubation of SMCs with iron(III) chloride showed the same pattern as the incubation with iron(II) gluconate, displayed in Fig. 1b for 6 and 24 h. A down-regulation was observed for both time points, dose-dependently down to 30%. Also the co-incubation with iron(III) chloride led to a decrease of the relative number of metabolically active cells (upper part of the figures, right y-axis).

The influence of Ferrlecit™ on human smooth muscle cells is displayed in Fig. 1c for 6 and 24 h. The metabolic activity decreased in a concentration range from 0.1 to 100 µg/ml time dependently below 75%. As shown for iron(II)-gluconate and iron(III)-chloride, Ferrlecit™ led to a decrease of vital cells dose-dependently for all indicated time points (upper graphs, right y-axis). Ferrlecit™ concentrations >100 µg/ml led to a strong increase of absorption at a wavelength of 450 nm. This increase depends on the strong brown colour and not of any cellular effects as control experiments without cells showed. Thus the values for metabolic activity obtained from concentrations more than 100 µg/ml are not valid and are therefore not depicted in Fig. 1c.

In a second set of experiments we analyzed the influence of soluble ferrous iron on the expression of LDL-R, HMGCS1 and FADS1 in human vascular smooth muscle cells using TaqMan® Real-time PCR. SMCs were co-incubated with iron(II) gluconate for 12 and 24 h at different concentrations (30, 50 100, 500 and 1000 µg/ml). As shown in Fig. 2a Fe(II) led to an increase of mRNA expression for LDL-R, HMGCS1 and FADS1 in a concentration dependent way after 12 and 24 h. Concentrations >500 µg/ml decreased gene expression for both time points, probably as a result of reduced metabolic activity as shown above. The most prominent effects were observed at a concentration of 500 µg/ml: LDL-R: $-\Delta\Delta C_t$: 1.33 ± 0.33 (12 h), 2.33 ± 0.25 (24 h); HMGCS1: $-\Delta\Delta C_t$: 1.81 ± 0.26 (12 h), 3.57 ± 3.36 (24 h); FADS1: $-\Delta\Delta C_t$: 1.23 ± 0.09 (12 h), 2.34 ± 0.30 (24 h). In this context HMGCS1 exhibited the strongest effects. These gene expression data confirmed the data obtained by Affymetrix analysis.

Furthermore, we analyzed the effects of soluble ferric iron (iron(III) chloride) towards the genes mentioned above. After 12 h no effects were detectable. The 24 h experiments gave evidence that concentrations of Fe(III) chloride greater than 100 µg/ml led to toxic effects as shown also by the metabolic data in Fig. 1b, resulting in low amounts of poor

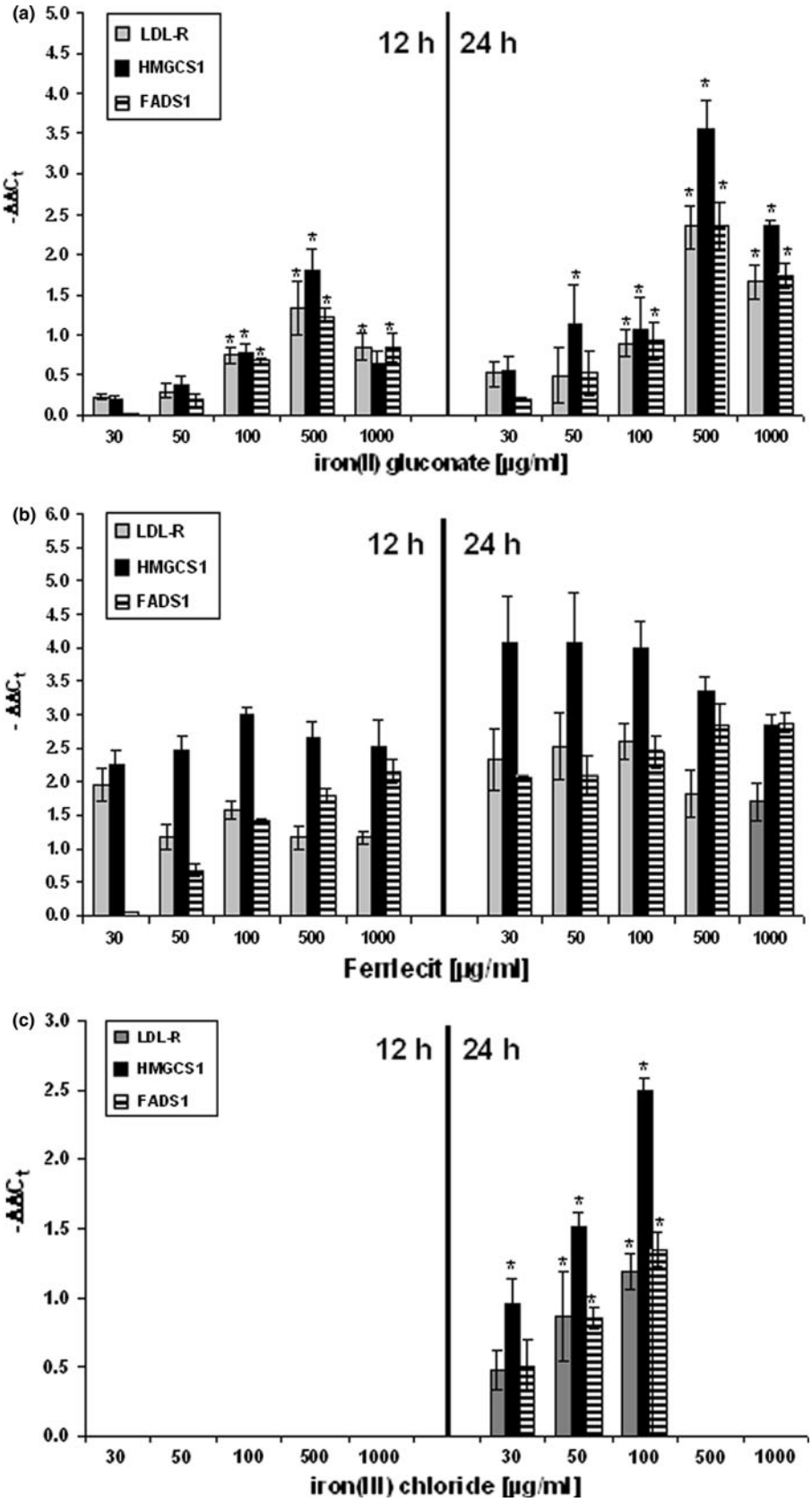

Fig. 2 Human vascular smooth muscle cells (4×10^5 each) were incubated with iron(II) gluconate (**a**), iron(III)-chloride (**b**) and Ferrlecit™ (**c**) in a concentration range from 30 to 1,000 µg/ml for 12 and 24 h. The gene expression of LDL-R, HMGCS1 and FADS1 was determined using TaqMan® Real-time-PCR. Significant differences in $-\Delta\Delta C_t$ are marked with an asterisk ($P < 0.05$)

quality RNA which was not sufficient for gene expression analysis. Reliable results were obtained only at concentrations from 30 to 100 μg/ml. Within this concentration range a significant up-regulation was observed for LDL-R ($-\Delta\Delta C_t$: 0.86 ± 0.32 (50 μg/ml), $-\Delta\Delta C_t$: 1.19 ± 0.12 (100 μg/ml); HMGCS1 ($-\Delta\Delta C_t$: 0.96 ± 0.18 (30 μg/ml), $-\Delta\Delta C_t$: 1.51 ± 0.11 (50 μg/ml), $-\Delta\Delta C_t$: 2.50 ± 0.09 (100 μg/ml) and FADS1 ($-\Delta\Delta C_t$: 0.85 ± 0.08 (50 μg/ml), $-\Delta\Delta C_t$: −1.35 ± 0.12 (100 μg/ml) as depicted in Fig. 2b.

In addition to soluble iron(III) we analyzed the influence of iron(III) in form of solid Fe_2O_3 in a gluconate complex (Ferrlecit™). Cell culture experiments using size-defined Fe_2O_3 micro-and nano-particles were not evaluable, since these particles agglutinate in aqueous environments. To rule out effects resulting from the preservative benzyl alcohol in the pharmaceutical formulation of Ferrlecit™ we co-incubated vascular smooth muscle cells with benzyl alcohol up to a 10-fold increase compared to its concentration in the drug. No influence on the expression of all three genes was observed.

The iron(III) concentration in the Fe_2O_3–gluconate complex is 12.5 mg/ml. As for the experiments with soluble iron, we evaluated the effects of Ferrlecit™ in a concentration range from 30 to 1,000 μg/ml (Fig. 2c). For the LDL-R a dose dependent up-regulation was observed after 24 h with a maximum at 100 μg/ml ($-\Delta\Delta C_t$: 2.6 ± 0.28). Higher concentrations resulted in a down-regulation ($-\Delta\Delta C_t$: 1.82 ± 0.36) for 500 μg/ml, and ($-\Delta\Delta C_t$: 1.69 ± 0.28) for 1000 μg/ml, respectively. For HMGCS1 the most prominent effects after 12 h were observed for 100 μg/ml ($-\Delta\Delta C_t$: 3.0 ± 0.09). After 24 h the maximum of expression was measured at a concentration of 100 μg/ml ($-\Delta\Delta C_t$: 4.0 ± 0.40), followed by a decrease to ($-\Delta\Delta C_t$: 3.34 ± 0.24) for 500 μg/ml and ($-\Delta\Delta C_t$: 2.85 ± 0.15) for 1,000 μg/ml. For FADS1 a dose-dependent up-regulation was observed for 12 and 24 h. The most prominent effects were measured for 1,000 μg/ml ($-\Delta\Delta C_t$: 2.15 ± 0.27 (12 h) and 2.88 ± 0.17 (24 h)).

To confirm the hypothesis that iron corrosion products cause the up-regulation of LDL-R, HMGCS1 and FADS1, SMCs were exposed to solid iron in form of twisted coils. After 24 h strong signs of solid corrosion products were observed as depicted in Fig. 3a. As shown in Fig. 3b the expression of all three genes was upregulated: LDL-R ($-\Delta\Delta C_t$: 1.37 ± 0.39), HMGCS1 ($-\Delta\Delta C_t$: 3.30 ± 0.34), FADS1 ($-\Delta\Delta C_t$: 3.63 ± 0.49).

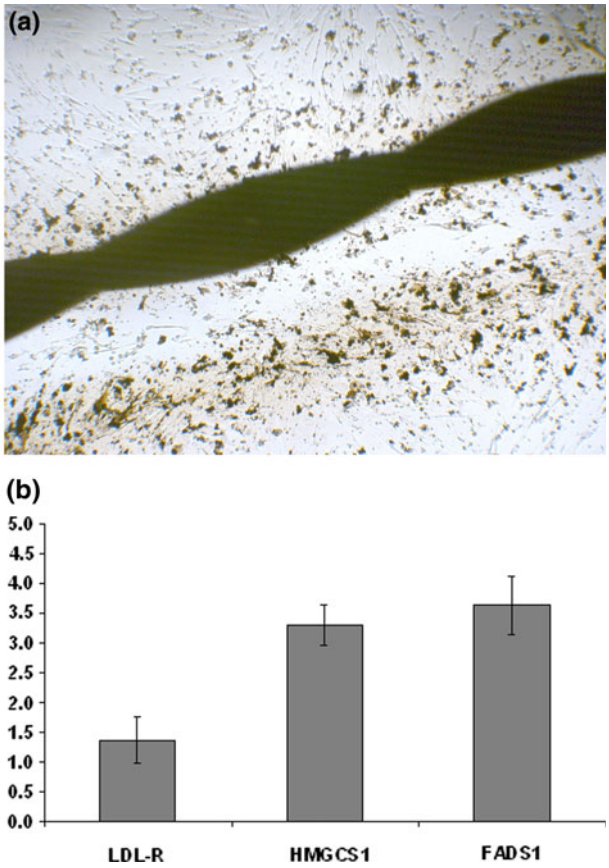

Fig. 3 Human vascular smooth muscle cells (4×10^5 each) were incubated with a twisted iron coil (6 cm lengths) for 24 h. The image (**a**) was recorded with 4× magnification. The gene expression of LDL-R, HMGCS1 and FADS1 was determined using TaqMan® Real-time-PCR (**b**). All indicated data points are significant ($P < 0.05$)

4 Discussion

Biodegradable stents are desirable for the treatment of obstructed vessels in growing pediatric patients and patients with peripheral or coronary artery disease [1]. Whereas polymeric stents have been evaluated with increased inflammatory and proliferative vascular responses, corrodible stents produced from iron and magnesium are promising candidates for biodegradable stents. In contrast to stents produced from magnesium alloys, iron stents exhibit excellent mechanical properties, little neointimal proliferation and little inflammation [1, 12].

In a novel approach of temporary stenting the first corrodible iron stent was introduced in 2001 using a rabbit model. Explanted iron stented vessels exhibited clearly visible signs of rust, although the mechanical integrity did not significantly decrease even after 24 months [12]. Rust was also found in surrounding tissues at the implantation site.

The corrosion of iron is a complex process, already outside physiological environments. The liberation of soluble ferrous iron is the first step of iron decomposition. In a multi step process iron(II) is oxidized to iron(III) (ferric form) in form of hydroxides and oxides.

$$Fe \rightarrow Fe^{2+} + 2e^{-}$$

$$H_2O + {}^1/_2O_2 + 2\ e^{-} \rightarrow 2OH^{-}$$

$$2\ Fe^{2+} + 4OH^{-} + {}^1/_2O_2 + H_2O \rightarrow 2Fe(OH)_3$$

$$Fe(OH)_3 \rightarrow FeO(OH) \times H_2O$$

$$2FeO(OH) \rightarrow Fe_2O_3 + H_2O$$

Theoretically the initially generated bi- and trivalent iron species react by partial deprivation of water to a mixture of iron(II)-oxide, iron(III)-oxide and crystal water, which is generally called rust.

$$xFe^{II}O \cdot yFe_2^{III}O_3 \cdot z\ H_2O(x, y, z = \text{positive ratios})$$

The respective composition of rust depends on several parameters, like pH values and salt concentrations. However, apart from theoretical considerations, the situation in vivo is much more complex. Since water is present in all biological environments the status of the equilibria (hydroxides–oxides) is not completely on the oxides side, so that the observed brown-coloured corrosion products in histological samples are composed of a mixture of highly non-soluble iron-hydroxides and oxides.

Systemic cytotoxic effects of iron are very unlikely because the amounts of iron in a typical stent (40 mg) are rather small in contrast to the whole-body iron load of 400–500 mg/l. Besides hemosiderin, ferritin is an important iron store. Approximately 20% of the total iron are bound in the bivalent form [13]. However, local iron concentrations may be higher and might interact with biological processes of the vasculature at the implantation site. Previous gene expression profiling studies demonstrated that gene clusters belonging to cell cycle regulation and cholesterol- and lipid-metabolism were up-regulated by soluble ferrous iron in human vascular smooth muscle cells [14]. This study focussed on genes related to cholesterol- and lipid-metabolism. We were able to confirm and extend these results by quantitative TaqMan® Real-time-PCR analysis over a wide concentration range for ferrous and ferric iron species.

The cellular functions of LDL-R, HMGCS1 and FADS1 are closely linked. The LDL-R gene family consists of cell surface proteins which are involved in receptor-mediated endocytosis of membrane bound low density lipoprotein (LDL) which is degradated in lysosomes [16]. The liberated cholesterol acts as a repressor for microsomal 3-hydroxy-3-methylglutaryl coenzyme A reductase (HMG-CoA), the rate-limiting step in cholesterol synthesis. This enzyme is regulated by a negative feedback mechanism mediated by sterol and non-sterol metabolites derived from mevalonate, the reaction product catalyzed by the reductase [17]. HMG-CoA is also the target of the widely available cholesterol lowering drugs known collectively as statins [18]. HMGCS1 is responsible for the condensation of acetyl coenzyme A (Ac-CoA) with acetoacetyl coenzyme A to 3-hydroxy-methylglutaryl-coenzyme A (HMG-CoA) which is than reduced to mevalonate by HMG-CoA reductase. This reaction pathway is essential for cholesterol and prenoid synthesis in mammals [19].

FADS1 belongs to the family of fatty acid desaturases (FADS). The unsaturation of fatty acids is performed by introduction of double bounds between well defined carbon atoms of the fatty acid acyl chain [20]. The reasons for the iron mediated up-regulation of genes involved in the cholesterol and lipid metabolism is not yet clear. All used iron-reagents induced gene expression within a broad concentration range, partially in a dose-dependent fashion, but it was obvious that the most prominent effects were observed after incubation with Ferrlecit™ [21], a commercially available drug used for the treatment of iron-deficiency, followed by iron(II)-gluconate and iron(III)-chloride. Also the incubation of smooth muscle cells with pure iron in form of twisted coils led to the induction of all three genes caused by bi- or trivalent corrosion products.

The effects of Fe(II) can be explained by its capability to replace other metal ions or by its reducing power. Fe(II) is oxidized to Fe(III) by cellular peroxides resulting in the formation of highly aggressive hydroxyl-radical species (Fenton reaction) [22, 23]. These radicals may react with a large group of biomolecules, e.g. membrane components [24, 25]. Disturbances in cellular membranes may lead to an increased cellular synthesis, since membrane bound cholesterol determines membrane fluidity and is a key factor for the function of membrane proteins [26, 27].

Under normal physiological conditions more than 99% of ferric iron is bound to the store proteins hemosiderin and ferritin—accumulation occurs mainly in secondary lysosomes. In acid environments or in the presence of reducing agents, e.g. ascorbic acid, NADPH, glutathione, free or bound ferric iron is reduced whereby formation of oxygen radicals and peroxidation of unsaturated fatty acids may occur.

The iron in form of the drug Ferrlecit™ can be considered as ferric (Fe_2O_3) "particles" in a gluconate complex embedded in a sucrose matrix with the stochiometrical formulation $[NaFe_2O_3(C_6H_{11}O_7)(C_{12}H_{22}O_{11})_5]_{n\ =\ 200}$ [28]. Several clinical studies showed that intravenously administered Ferrlecit™ leads to an increase of oxidative stress in form of reactive oxygen species [29, 30].

We attempted to perform cell culture experiments using Fe_2O_3 micro- and nanoparticles of different sizes (<50 μm and <50 nm), however, due to the limited bioavailability of the nanoparticles caused by aggregation in aqueous environments, these experiments were abandoned. SMC cell cultures exposed to solid iron coils exhibited clearly visible brown coloured corrosion products, probably rust components as $Fe(OH)_3/Fe_2O_3$. Gene expressions of LDL-R,

HMGCS1 and FADS1 in these experiments were also significantly up-regulated. It can be speculated, that the Fe_2O_3–gluconate complex of the Ferrlecit^{TM} formulation acts in the same way as the rust components. The increased bioavailability of iron in the Ferrlecit^{TM} formulation, however, leads to a pronounced effect.

Our data show, that soluble and insoluble iron species both in ferrous as well as in ferric forms lead to an induction of genes involved in cholesterol- and fatty acid metabolism. The most prominent effects, especially for HMGCS1, the precursor in cholesterol synthesis, were detected for the sucrose embedded Fe_2O_3–gluconate (Ferrlecit^{TM}) complex.

Cholesterol is known to be involved in the development of atherosclerotic plaques [31]. A currently published case report dealing with stented coronary vessels revealed that cholesterol containing atherosclerotic plaques also occurred within the boundaries of two bare metal stents even after 9 years [32]. These plaques may have a natural origin like plaques in unstented vessels. Since cholesterol in its different forms is abundant in the body there is actually no evidence that the plaques are related to corrosion products from the stents.

From the presented data it is not possible to determine the inducing agent for the expression of LDL-R, HMGCS1 and FADS1.We assume that ferrous as well as ferric iron act by the generation of highly reactive oxygen species. Although systemic effects from corrosion products in vivo can be excluded [1, 12], local effects at the implantation site are possible. The detected effects on the expression of genes related to the cholesterol synthesis may raise questions on the increased development of atherosclerotic plaques at implantation site of the iron stent. However, these effects were not observed after the implantation of slowly corroding iron stents into the aorta of New Zealand white rabbits and minipigs [1, 12]. More rapidly corroding iron-based alloys, however, may exhibit more pronounced effects on atherosclerosis and have to be observed for the occurrence of plaque formation after their implantation into the vasculature.

5 Conclusion

We investigated the effects of soluble bi- and trivalent iron compounds on the expression of genes involved in the cholesterol synthesis and fatty acid metabolism in human smooth muscle cells. It could be shown by quantitative TaqMan® Real-time PCR that soluble and solid forms of bi- and trivalent iron led to an induction of cholesterol- and fatty acid metabolism related genes, probably caused by iron related generation of highly reactive oxygen species. Further experiments will determine, whether expression of the described genes induced by the implantation of corrodible iron stents may lead to the generation of atherosclerotic plaques within the stent.

References

1. Peuster M, Hesse C, Schloo T, Fink C, Beerbaum P, von Schnakenburg C. Long-term biocompatibility of a corrodible peripheral iron stent in the porcine descending aorta. Biomaterials. 2006;27:4955–62.
2. Waksman R, Pakala R, Baffour R, Seabron R, Hellinga D, Tio FO. Short-term effects of biocorrodible iron stents in porcine coronary arteries. J Interv Cardiol. 2008;21:15–20.
3. Ramcharitar S, Serruys PW. Fully biodegradable coronary stents: progress to date. Am J Cardiovasc Drugs. 2008;8:305–14.
4. Heintz C, Riepe G, Birken L, Kaiser E, Chakfé N, Morlock M, et al. Corroded nitinol wires in explanted aortic endografts: an important mechanism of failure? J Endovasc Ther. 2001;8:248–53.
5. Reclaru L, Lerf R, Eschler PY, Meyer JM. Corrosion behavior of a welded stainless-steel orthopedic implant. Biomaterials. 2001;22:269–79.
6. Peuster M, Fink C, von Schnakenburg C, Hausdorf G. Dissolution of tungsten coils does not produce systemic toxicity, but leads to elevated levels of tungsten in the serum and recanalization of the previously occluded vessel. Cardiol Young. 2002;12:229–35.
7. Ryan MP, Williams DE, Chater RJ, Hutton BM, McPhail DS. Why stainless steel corrodes. Nature. 2003;415:770–4.
8. Brown DA, Lee EW, Loh CT, Kee ST. A new wave in treatment of vascular occlusive disease: biodegradable stents–clinical experience and scientific principles. J Vasc Interv Radiol. 2009;20:315–24.
9. Heublein B, Rohde R, Kaese V, Niemeyer M, Hartung W, Haverich A. Biocorrosion of magnesium alloys: a new principle in cardiovascular implant technology? Heart. 2003;89:651–6.
10. Drynda A, Hassel T, Hoehn R, Perz A, Bach FW, Peuster M. Development and biocompatibility of a novel corrodible fluoride-coated magnesium-calcium alloy with improved degradation kinetics and adequate mechanical properties for cardiovascular applications. J Biomed Mater Res A. 2009. Epub ahead of print.
11. Kraft CN, Diedrich O, Burian B, Schmitt O, Wimmer MA. Microvascular response of striated muscle to metal debris. A comparative in vivo study with titanium and stainless steel. J Bone Joint Surg Br. 2003;85:133–41.
12. Peuster M, Wohlsein P, Brügmann M, Ehlerding M, Seidler K, Fink C, et al. A novel approach to temporary stenting: degradable cardiovascular stents produced from corrodible metal—results 6–18 months after implantation into New Zealand white rabbits. Heart. 2001;86:563–9.
13. Andrews NC. Disorders of iron metabolism. N Engl J Med. 1999;341:1986–95. erratum in: N Engl J Med. 2000;342:364.
14. Mueller PP, May T, Perz A, Hauser H, Peuster M. Control of smooth muscle cell proliferation by ferrous iron. Biomaterials. 2006;27:2193–200.
15. Jaffe EA, Nachman RL, Becker CG, Minick CR. Culture of human endothelial cells derived from umbilical veins. Identification by morphologic and immunologic criteria. J Clin Invest. 1973;52:2745–6.
16. Brown MS, Goldstein JL. Receptor-mediated endocytosis: insights from the lipoprotein receptor system. Proc Natl Acad Sci USA. 1979;76:3330–7.
17. Vock C, Döring F, Nitz I. Transcriptional regulation of HMG-CoA synthase and HMG-CoA reductase genes by human ACBP. Cell Physiol Biochem. 2008;22:515–24.

18. Greenfeder S. Emerging strategies and agents to lower cardiovascular risk by increasing high density lipoprotein cholesterol levels. Curr Med Chem. 2009;16:144–56.
19. Rokosz LL, Boulton DA, Butkiewicz EA, Sanyal G, Cueto MA, Lachance Pa, et al. Human cytoplasmic 3-hydroxy-3-methylglutaryl coenzyme A synthase: expression, purification, and characterization of recombinant wild-type and Cys129 mutant enzymes. Arch Biochem Biophys. 1994;312:1–13.
20. Martinelli N, Girelli D, Malerba G, Guarini P, Illig T, Trabetti E, et al. FADS genotypes and desaturase activity estimated by the ratio of arachidonic acid to linoleic acid are associated with inflammation and coronary artery disease. Am J Clin Nutr. 2008;88:941–9.
21. Gotloib L, Silverberg D, Fudin R, Shostak A. Iron deficiency is a common cause of anemia in chronic kidney disease and can often be corrected with intravenous iron. J Nephrol. 2006;19:161–7.
22. Farber JL. Mechanisms of cell injury by activated oxygen species. Environ Health Perspect. 1994;102(Suppl 10):17–24.
23. Marnett LJ. Oxy radicals, lipid peroxidation and DNA damage. Toxicology. 2002;181–182:219–22.
24. Abdalla DS, Campa A, Monteiro HP. Low density lipoprotein oxidation by stimulated neutrophils and ferritin. Atherosclerosis. 1992;97:149–59.
25. Enright HU, Miller WJ, Hebbel RP. Nucleosomal histone protein protects DNA from iron-mediated damage. Nucleic Acids Res. 1992;20:3341–6.
26. Bernotti S, Seidman E, Sinnett D, Brunet S, Dionne S, Delvin E, et al. Inflammatory reaction without endogenous antioxidant response in Caco-2 cells exposed to iron/ascorbate-mediated lipid peroxidation. Am J Physiol Gastrointest Liver Physiol. 2003;285:G898–906.
27. Suwalsky M, Martínez F, Cárdenas H, Grzyb J, Strzalka K. Iron affects the structure of cell membrane molecular models. Chem Phys Lipids. 2005;134:69–77.
28. http://pi.watson.com/data_stream.asp?product_group=1235&p=pi&language=E Watson Pharma, 09/2006.
29. Pai AB, Boyd AV, McQuade CR, Harford A, Norenberg JP, Zager PG. Comparison of oxidative stress markers after intravenous administration of iron dextran, sodium ferric gluconate, and iron sucrose in patients undergoing hemodialysis. Pharmacotherapy. 2007;27:343–50.
30. de Vecchi AF, Novembrino C, Lonati S, Ippolito S, Bamonti F. Two different modalities of iron gluconate i.v. administration: effects on iron, oxidative and inflammatory status in peritoneal dialysis patients. Nephrol Dial Transplant. 2007;22:1709–13.
31. Kolodgie FD, Burke AP, Nakazawa G, Cheng Q, Xu X, Virmani R. Free cholesterol in atherosclerotic plaques: where does it come from? Curr Opin Lipidol. 2007;18:500–7.
32. Agostoni P, Vermeersch P, Knaapen M, Verheye S. Stent thrombosis is not always stent thrombosis: de novo atherosclerosis in a stented coronary segment. Int J Cardiol. 2009. Epub ahead of print.